A SYSTEMATIC STUDY OF ACOUSTIC EMISSION FROM NUCLEAR GRAPHITES

G.B. NEIGHBOUR*, B. McENANEY
School of Materials Science, Bath University,
Bath, United Kingdom

Abstract

Acoustic emission (AE) monitoring has been identified as a possible method to determine internal stresses in nuclear graphites using the Kaiser effect, *i.e.*, on stressing a graphite that has been subject to a prior stress, the onset of AE occurs at the previous peak stress. For three nuclear graphites (PGA, IM1-24 and VNEC), AE was monitored during both monotonic and cyclic loading to failure in tensile, compressive and flexural test modes. For unirradiated graphites, the Kaiser effect was not found in cyclic loading, but a Felicity effect was observed, *i.e.*, the onset of AE occurred below the previously applied peak stress. The Felicity effect was attributed to time-dependent relaxation and recovery processes and was characterised using a new parameter, the Recovery ratio. It was shown that AE can be used to monitor creep strain and creep recovery in graphites at zero load. The AE-time responses from these experiments were fitted to equations similar to those used for creep strain-time at elevated temperatures. The number of AE counts from irradiated graphites were greater than those from unirradiated graphites, subject to similar stresses, due to increases in porosity caused by radiolytic oxidation. A Felicity effect was also observed on cyclic loading of irradiated graphites, but no evidence for a Kaiser effect was found for irradiated graphites loaded monotonically to failure. Thus internal stresses in irradiated graphites could not be measured using AE. This was attributed to relaxation and recovery processes that occur between removing the irradiated graphite from the reactor and AE testing. This work indicated that AE monitoring is not a suitable technique for measuring internal stresses in irradiated graphite.

1. INTRODUCTION

Both Magnox and AGR reactors contain a core of graphite moderator bricks whose prime function is to slow down fast neutrons to thermal energies; additionally, the core also serves as a major structural material. Changes in dimensions and reduction in strength of moderator bricks, resulting from neutron irradiation and radiolytic oxidation, give rise to complex residual stresses that in principle may lead to failure of moderator bricks. Failure could cause severe problems such as the jamming of a fuel stringer in the channel, or blocking the insertion of control rods. For these reasons, there is a clear need for methods to monitor residual stresses within the reactor core and acoustic emission (AE) has been identified as a potential method, using the Kaiser Effect [1-4]. This Effect occurs when AE is generated only when an applied stress exceeds the previous peak stress.

Previous studies of AE from graphites have shown that: (i) AE from graphites increases with coarseness of microstructural texture [5, 6]; (ii) AE from annealed, irradiated graphites is greater than from an unirradiated graphite of the same type [7]. Several studies of AE from graphites report a Kaiser Effect [1-4]. Some recent studies [8-10] have reported deviations from the Kaiser Effect, attributed to reversed plastic slip deformation on unloading. Prestressing to 90% σ_f has little effect on AE, but significantly more AE was found after annealing [11]. Recovery was attributed to slip deformation from heat treatment and to recovery of cleavage between basal planes.

This paper presents an overview of an extensive study which was initiated to determine the suitability of AE for monitoring residual stresses in core graphites [12-15].

* Present address: Fuel Performance Group, AEA Technology,
Windscale, Cumbria, United Kingdom

2. EXPERIMENTAL

2.1 Materials

Two graphites used in this work were PGA and IM1-24 which are the moderator graphites for Magnox and AGR, respectively. For some work, VNEC, a candidate sleeve material, was also used. Details of the microstructure of these materials are in [12].

2.2 Mechanical Tests and Acoustic Emission

All measurements, except those for irradiated graphite, were made using an Instron 1195; stress cycling experiments were carried out using a cross head speed of 0.5 mm per min; the AE measurement technique is described in [13] and for irradiated graphites in [15].

2.3 Experimental Programme

Brief descriptions of the major components of the experimental programme are given below; details are in [13-15].

(a) Monotonic Loading AE responses were measured from unirradiated nuclear graphite monotonically loaded to failure in tension and flexure. AE responses from compression loading to failure were not obtained to avoid damage to the AE transducer.

(b) Single-Mode Cyclic Loading AE responses were monitored from unirradiated nuclear graphite cyclically loaded in either tension, compression or flexure to 5 MPa, unloaded, re-loaded to 10 MPa, unloaded and re-loaded to 15 MPa. Some mixed-mode cyclic loading experiments were made [12], but these will not be considered in this paper. These experiments were designed to test for the presence of the Kaiser Effect.

(c) Time Dependent AE Responses These experiments were designed to monitor the effect of recovery processes on AE. Two series of tests were undertaken at ambient temperature. (i) Batches of six IM1-24 specimens were subjected to two compressive load cycles: (a) loaded to 30 MPa and unloaded; and, (b) after time, t, reloaded to 40 MPa and then unloaded, where t was 0, 10^0, 10^1, 10^2, 10^3, 10^4 and 10^5 minutes. (ii) AE was recorded from both PGA and IM1-24 graphite specimens subjected to two types of tensile and compressive load patterns: (a) monotonically loaded to stress, σ_1, unloaded and the AE monitored for a time, t, at zero stress; and, (b) monotonically loaded to stress, σ_1, and AE monitored for time, t, at constant strain before unloading to zero stress; t was approximately 16 hours in all cases. For PGA and IM1-24 graphite, σ_1 was 70% and 80% of the failure strength, respectively. A lower value of σ_1 was used for PGA since the probability of failure was greater.

(d) Irradiated Nuclear Graphites AE responses were obtained from both unirradiated and irradiated Gilsocarbon sleeve graphite subjected to two loading patterns: (i) three consecutive load-unload cycles to 5 MPa, 10 MPa and to failure in flexure (3 pt bend), and (ii) monotonically increasing flexural load to failure. The first set of experiments were designed as tests for the Kaiser Effect and the second loading pattern was designed to examine the extent (if any) of the Kaiser Effect arising from internal stresses resulting from reactor conditions.

3. RESULTS AND DISCUSSION

3.1 Mechanical Properties

Mechanical properties of the three graphites are summarised in Table 1. PGA is the weakest graphite in all testing modes. The compressive strength of IM1-24 is greater than those of the other two graphites due to the inhibition of shear deformation by the Gilsocarbon filler particles, whereas pitchcoke filler particles facilitate shear for the other two graphites. More detailed consideration of these data is in [12-14].

TABLE 1 : Static Mechanical Properties of PGA, IM1-24 and VNEC Nuclear Graphites.

	PGA			IM1-24			VNEC		
	Mean	**S.D.**	**n**	**Mean**	**S.D.**	**n**	**Mean**	**S.D.**	**n**
Density / g cm^{-3}	1.739	0.014	10	1.819	0.005	10	1.807	0.016	10
Fractional Porosity / %	23.05			19.51			20.05		
Dynamic Modulus / GPa	14.14	1.42	10	10.90	0.25	10	11.72	0.90	10
Tensile Strength / MPa	11.04	1.00	6	14.22	1.53	7	14.33	2.36	5
Compressive Strength/MPa	34.50	5.80	6	72.15	3.69	9	51.98	5.01	6
Flexural Strength / MPa	20.11	2.98	10	25.81	2.35	10	28.52	3.85	5

3.2 Acoustic Emission

(a) AE Responses From Monotonic Loading

The AE responses from the three graphites subjected to monotonic loading to failure in tension, Figure 1, show that the graphites are critically active, *i.e.*, the slope of the plot of cumulative AE event counts, ΣN, versus stress, increases progressively with stress. For all graphites, AE starts at the lowest applied stress in contrast to some previous studies [e.g. 3] where an onset stress was observed. The detection of AE at low stress in this work is attributed to the improved technology and sensitivity of the AE detection system compared with earlier work.

In both tension and flexure, the ratio of ΣN at failure, for PGA, VNEC and IM1-24 is approximately 10:5:1, Table 2. The high value of ΣN for PGA can be related to its coarser texture compared to the other two graphites [5,6]. Although flexural strengths are greater than tensile strengths, Table 1, values of ΣN in flexure are smaller than those in tension for all three graphites, Table 2. This is because the stressed volume in flexure is much smaller than in tension. As a consequence, the process zone, in which AE generating processes occur, is confined to a localised region of high tensile stress (although a small number of AE events are probably also generated in the region of the test specimen subject to compressive stresses). This suggests that flexural loading is likely to be less suitable for AE monitoring than is tensile testing.

TABLE 2 : Mean ΣN (± 1 s.d.) at Failure For Monotonic Loading of Three Nuclear Graphites in Tension and Flexure (the number of specimens used are in parenthesis).

	PGA	IM1-24	VNEC
ΣN at σ_f (tension)	66752 ± 9263 (5)	6018 ± 1861 (6)	33368 ± 8947 (5)
ΣN at σ_f (flexure)	20779 ± 6296 (10)	2827 ± 1057 (10)	9508 ± 3049 (5)

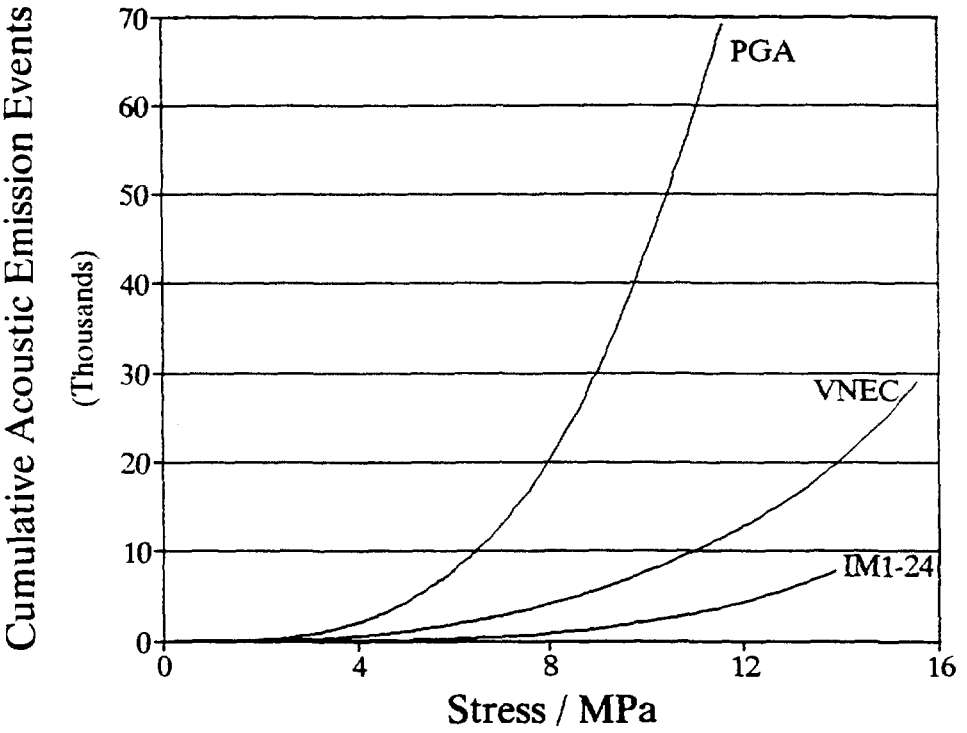

FIGURE 1: Typical AE responses for the three graphites monotonically loaded to failure in tension.

(b) AE Responses From Single-Mode Cyclic Loading

Figure 2 presents examples of AE responses from cyclic loading in compression for both PGA and IM1-24 graphites. The AE response for IM1-24 is typical of all cyclic stressing for all graphites in all modes except PGA in compression. On the first cycle, ΣN increases progressively from zero stress, and in subsequent cycles, AE resumes at stresses which approach, but are less than the previous peak stress, *i.e.* a Kaiser Effect is not observed. These AE responses are examples of the Felicity Effect. (An explanation for the behaviour of PGA graphite in compression is given in [12].)

The Felicity Effect may be associated with recovery processes occurring during unloading between cycles and may be characterised by the Felicity Ratio, F, which is the ratio of the onset stress of AE, σ_o, to the previous maximum stress experienced by the specimen, σ_p, *i.e.*, $F = \sigma_o / \sigma_p$. (The Felicity Effect was first reported for cyclic stressing of composite materials [16].) The Felicity Ratio has two main disadvantages as a tool to characterise AE on cyclic loading: (i) it does not take account of the amount of AE prior to the previous maximum stress level, and (ii) the onset stress is difficult to determine and may require an arbitrary threshold to be set, and thus lead to spurious results. Therefore, a new parameter called the Recovery Ratio, B, was proposed; B is defined as the ratio of the cumulative AE event count (N_2) on cycle (n+1) at the previous peak stress and the cumulative AE event count (N_1) at the peak stress on cycle n, *i.e.*, $B = N_2 / N_1$. If a Kaiser Effect occurs, then $B = 0$, but if a Felicity Effect occurs, then $0<B<1$. The Recovery Ratio is a precise measurement, and it does not depend on arbitrary or calculated thresholds set by the operator, as is the case for F.

B values were calculated at 5 and 10 MPa for all three graphites after three consecutive load cycles. Mean values of B for all graphites in all testing modes range from 0.04 to 0.16. Thus, the number of AE events generated on the (n+1) cycle before the previous peak stress is a significant fraction of the ΣN at the previous peak stress. In all but one case, $B>0$ (95% confidence) confirming that the Kaiser Effect is not observed in these cases.

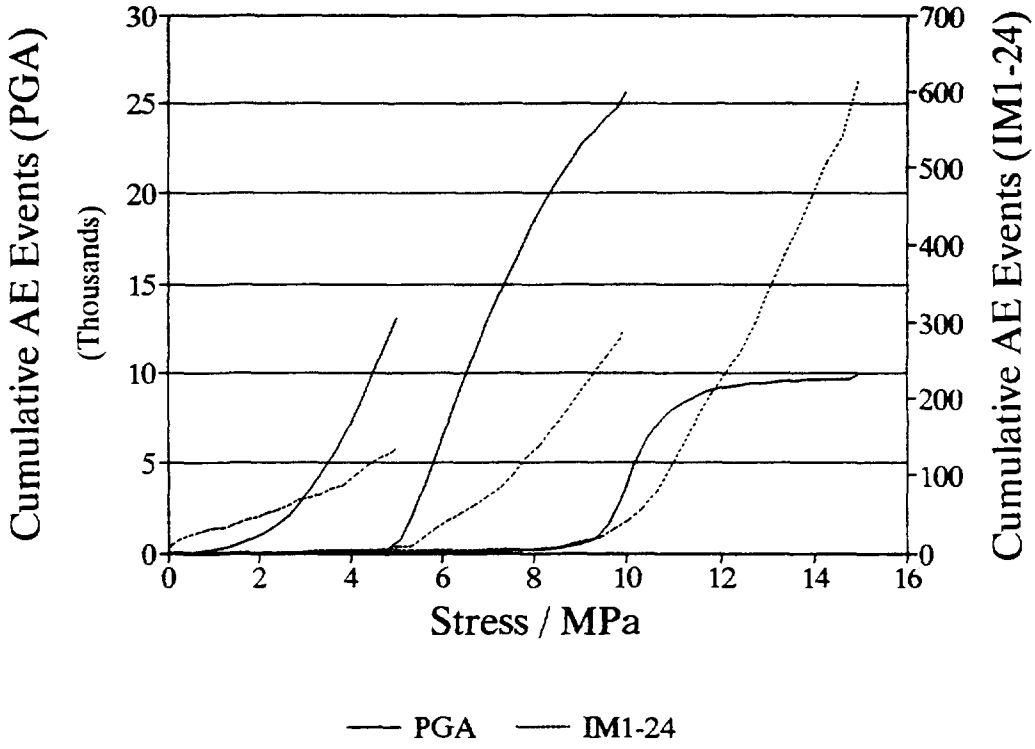

FIGURE 2: Typical cyclic compressive AE responses (PGA and IM1-24).

TABLE 3 : Recovery Ratios, B (± 1 S.D.) at 5 and 10 MPa For Three Nuclear Graphites in Tension, Compression and Flexure (where n is the number of samples)

Recovery Ratio, B							
		PGA		IM1-24		VNEC	
		5 MPa	10 MPa	5 MPa	10 MPa	5 MPa	10 MPa
Tension	Mean	0.097	0.072	0.066	0.088	0.111	0.076
	s.d.	0.026	0.009	0.035	0.016	0.045	0.013
	n	6	6	10	10	5	5
Compression	Mean	0.041	0.138	0.058	0.122	0.083	0.086
	s.d.	0.021	0.104	0.023	0.032	0.024	0.025
	n	10	10	9	8	4	5
Flexure	Mean	0.092	0.090	0.124	0.153	0.161	0.091
	s.d.	0.064	0.032	0.133	0.081	0.152	0.063
	n	10	10	10	10	5	5

In cyclic compressive loading, the mean B value at 10 MPa for all three graphites is greater than at 5 MPa (although only slightly greater for VNEC) suggesting that the increased pre-stress causes an increasing extent of recovery on unloading, Table 3. This result is consistent with the postulate that basal plane shear (which is the dominant initial response of graphites to compressive loading) is reversible to some extent upon unloading as a result of back-stresses [9]. This trend is not found for cyclic tensile loading where the mean values of B at 5 and 10 MPa are not significantly different from each other, Table 3. This may indicate that on cyclic tensile loading to 5 and 10 MPa, there is a greater proportion of microcracking, which is non-recoverable, than there is in compressive loading. This explanation is plausible when the difference in compressive and tensile failure modes for these graphites is considered, together with the fact that 10 MPa is a higher fraction of the tensile failure stress than it is of the compressive failure stress. Thus, although B values are subject to large

scatter, these results are in broad agreement with the postulate that microcracking is a non-recoverable process and that basal plane shear is reversible on unloading, as suggested by [9] and in a theoretical model by [17].

(c) Time-Dependent AE Responses

The presence of the Felicity Effect in nuclear graphites can be attributed to recovery processes of which at least two factors may contribute: (i) recovery during unloading due to some reversal of intercrystalline shear, and (ii) relaxation of residual strain at zero stress which is a function of time at zero stress. To determine the extent of time-dependent processes two types of test were undertaken.

The first set of tests attempted to quantify the relationship between the "recovery" in nuclear graphites, shown by the B value, and the time at zero stress between successive load cycles. Figure 3 (a) and (b) present typical examples of AE responses for zero time and 10^5 minutes between two successive load cycles, respectively. For t=0, the response is similar to that found for compressive cyclic loading discussed earlier, Figure 2. However, for $t=10^5$, the AE response for a second load cycle after a period of time at zero load differs from that for immediate reloading. On reloading there is a short rise in ΣN at low stress, and then ΣN remained constant until the previous peak stress was approached, when ΣN begins to rise sharply. Since the increase in ΣN after time at zero load occurs below 10 MPa, a modified Recovery ratio, B' was defined as the ratio of ΣN values on the 1st and 2nd cycles at 10 MPa. The increase in mean B' values with t was fitted to an empirical, semi-logarithmic equation:

$$B' = 56.7 \times 10^{-3} \log_{10} t + 0.034 \qquad \text{Eqn. (1)}$$

with a Pearson's r coefficient of 0.91. The initial release of AE at the low stress presumably relates to easy deformation processes which increase with time at zero load between load cycles. Since these events do not occur if a specimen is immediately re-loaded, then they must be related to the recovery of the specimen.

In the second type of test, AE was monitored from specimens that were stressed under constant strain conditions or specimens that were pre-stressed and then held at zero stress. The ΣN-time curves in both types of test were similar in shape. Figure 4 presents an example of ΣN versus t for PGA in compression at constant strain. The curve shows initially a rapid rise in ΣN after which the rate of AE generation gradually decreases with time, although AE is still being generated even after ~16 hours. The shape of the curve of ΣN vs t suggest that the AE is generated by microstructural events, and not from background noise since in the latter case the rate of AE generation would be approximately constant. The curve shape also suggests that eventually ΣN will reach a limiting value, *i.e.*, there is a maximum amount of "recovery" that can occur.

The AE generated during the 16h period is a small fraction of the AE generated upon initial loading. For example, for those specimens monitored at constant strain, ΣN after 10^3 minutes increased by between 0.8 and 3.4% of ΣN at the start of monitoring. The AE responses from graphite specimens monitored at zero stress after a load cycle was similar to the response at constant strain but the AE generated was much less and varied between <0.1% to 1.4% of the ΣN immediately after unloading. It was shown in the stress cycling experiments presented earlier, Table 3, that the number of AE events generated on reloading was ~10% of the AE events generated at the previous peak stress, and these were considered to be the result of recovery mechanisms. These experiments showed the

number of AE events generated at zero stress after a previous load are less than 2% of AE events generated at the previous peak stress. This suggests that the relaxation processes which occur at zero stress are sufficient to cause "new" AE events on reloading polycrystalline graphites.

Davidson and Losty [18] showed for a range of carbon and graphites, including reactor graphites, that at a given stress and temperature in the range 1000-2000°C primary creep strain, ε_t, was described by an equation of the form:

$$\varepsilon_t = A + k \log t \qquad \text{Eqn. (2)}$$

where A and k are constants. Davidson and Losty also suggested that creep strain recovery above 1500°C followed a similar logarithmic form. Andrew *et al.* [1] studied creep of graphites at ambient temperature and they showed that permanent set on unloading increased logarithmically with time of loading. They also demonstrated that there was some recovery on unloading with the permanent set decreasing with time at zero stress. It may be noted that the increase in the Recovery Ratio, B', with time, Eqn (1), is of similar form to Eqn (2).

It is possible to relate the AE response curve in Figure 4 to Eqn (2) as follows. AE occurs as a result of abrupt relaxation mechanisms. If each localised creep mechanism consists of abrupt increments of local creep strain, $\Delta\varepsilon$, and each increment acts as an AE source, then the sum of AE events at time, t, ΣN_t, is directly related to the accumulation of creep strain increments, *i.e.*, $\Sigma N_t = f(\Sigma\Delta\varepsilon) = f(\varepsilon_t)$. If it is further assumed that secondary creep at ambient temperature is negligible (as seems reasonable), then the ΣN - time curves for constant strain can be related to Eqn. (2):

$$\Sigma N_t = \Sigma N_0 + k_{ae} \log t \qquad \text{Eqn. (3)}$$

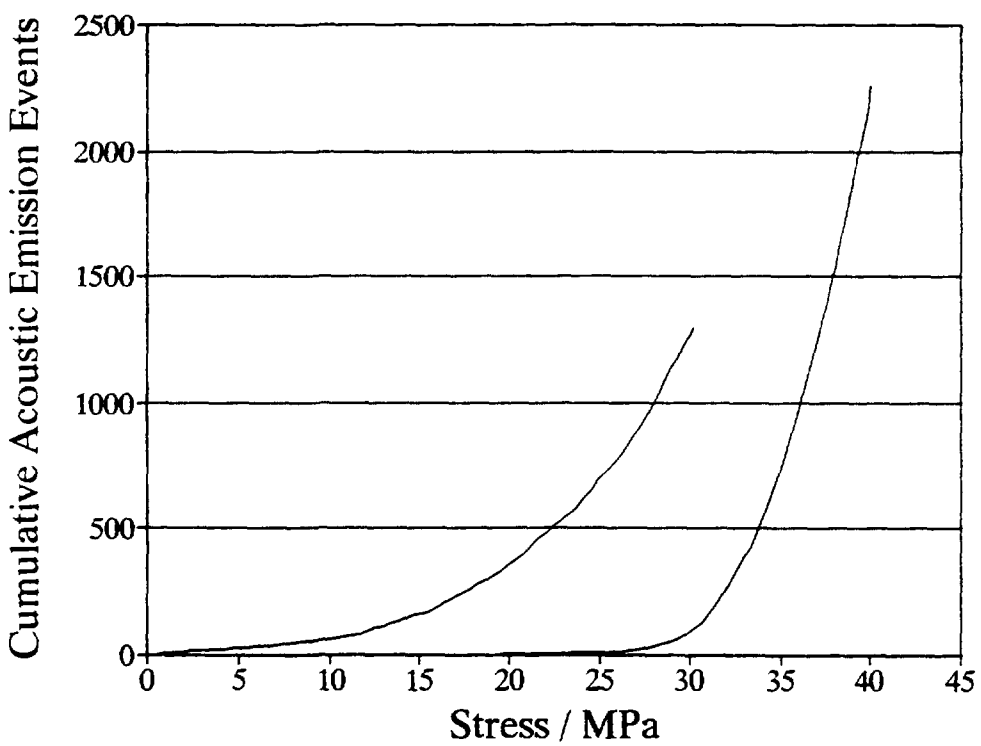

FIGURE 3 (a): Typical AE Response from IM1-24 graphite subject to two compressive load cycles where the time between each cycle is zero.

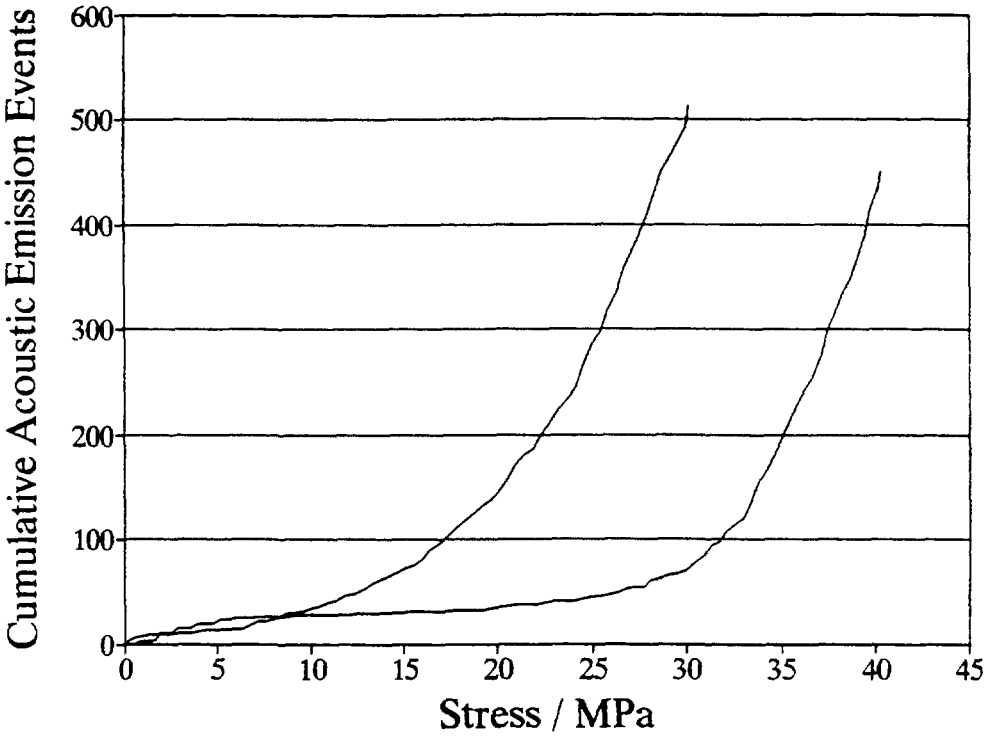

FIGURE 3 (b): Typical AE Response from IM1-24 graphite subject to two compressive load cycles where the time between each cycle is 10^5 minutes.

where ΣN_0 represents the cumulative AE event count due to the instantaneous load at t= 0 and k_{ae} is a constant similar to k in Eqn. (2). For those specimens which were subjected to a load cycle and the AE monitored at zero stress, the AE generated may be attributed to creep recovery mechanisms, and therefore in a similar manner to AE generated at constant strain, the cumulative AE event count after unloading at time t, $\Sigma N_t'$ may be expected to fit a function similar to Eqn. (3):

$$\Sigma N_t' = \Sigma N_0' + k_{ae}' \log t \qquad \text{Eqn. (4)}$$

where $\Sigma N_0'$ is the cumulative AE event count immediately after unloading, k_{ae}' is a constant similar to k_{ae}. Using this approach, a model creep curve can be obtained which closely fits the experimental AE data, Figure 4.

These results indicate at constant strain, thermally-activated creep driven by the strain energy may cause further slip of basal planes, and extension of existing stress-concentrating cracks and flaws, thus giving rise to AE. At zero stress after a load cycle, residual strain energy triggers AE events by reverse plastic deformation, leading to recovery. Presumably, the residual strain energy is concentrated as localised tensile and compressive micro-stresses (which average zero over the whole specimen). The extent of creep recovery is less in tension than in compression, suggesting an important component of creep recovery is reversal of shear deformation as a result of back-stresses due to boundary restraint [9]. Other possible sources of AE may be due to frictional effects at grain boundaries or at crack surfaces. A more detailed discussion of this subject is in [12, 14].

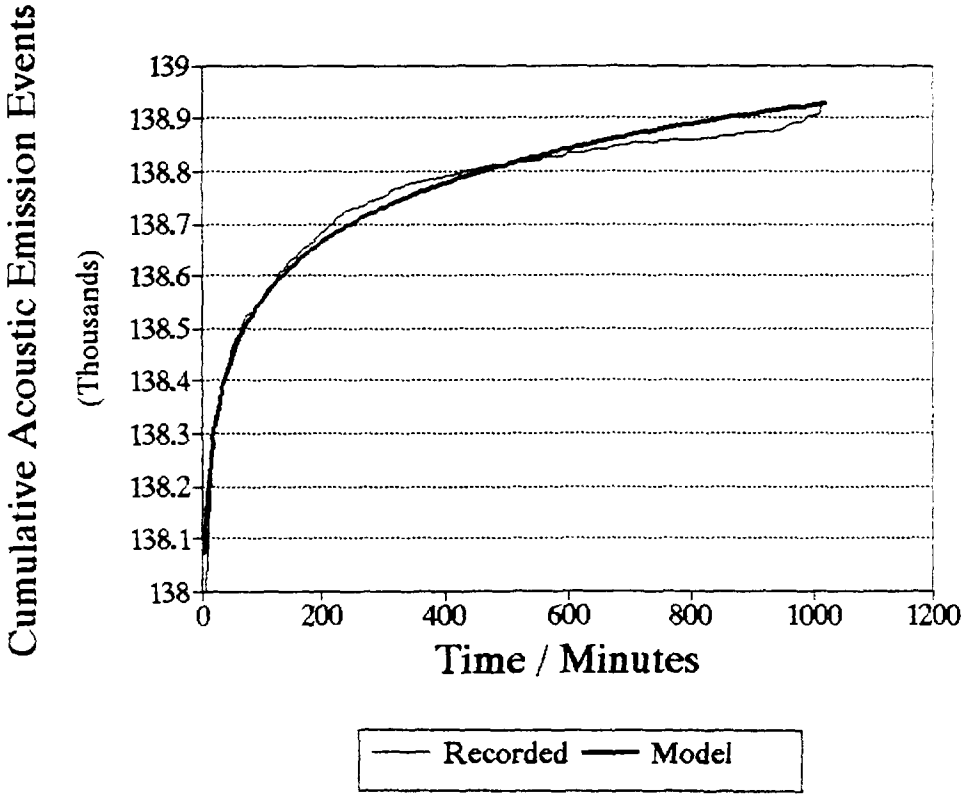

FIGURE 4: A comparison of a typical experimentally-recorded AE-time curve for PGA graphite subject to compressive strain (initial stress = 24.2 MPa) with a model curve calculated from Eqn. [3].

(e) AE Responses From Irradiated Nuclear Graphite

AE responses were obtained from irradiated graphite from Element 4 and 7 of a Gilsocarbon AGR fuel sleeve discharged after a full lifetime. AE responses from irradiated graphite (Figure 5) subjected to consecutive load cycles to 5 MPa, 10 MPa and then failure showed that the onset of AE is at the start of loading, *i.e.* a Felicity Effect was observed. The second load cycle is similar to that found for unirradiated graphite, but the AE clearly starts at zero stress. However, for most irradiated graphite samples, the third load cycle, differs from the usual response from unirradiated graphites because more AE is generated than in the second cycle until just prior to the previous maximum stress; this leads to high values of the Recovery ratio, B $\approx$ 0.5-1.0. However, for each load cycle the AE response showed a change in gradient at stresses approximately equal to that of the previous stress level.

The strength of the irradiated material is much less than that of the unirradiated material, Table 4, indicating that the effects of radiolytic oxidation greatly outweigh those of neutron hardening. Table 4 also shows, for all load cycles, that the ΣN values for irradiated graphites are significantly greater than for unirradiated graphite (95% significance). Higher AE for irradiated graphites is probably due to the development of porosity following radiolytic oxidation. AE responses from irradiated graphite samples monotonically loaded to failure, Figure 6, show an initial sharp rise and then a more gradual increase in ΣN to failure. The onset of AE occurs at zero stress, and at no point do ΣN values increase abruptly with increasing stresses. Therefore, AE responses from irradiated graphite did not show any evidence of a Felicity effect caused by internal stresses induced by the reactor environment.

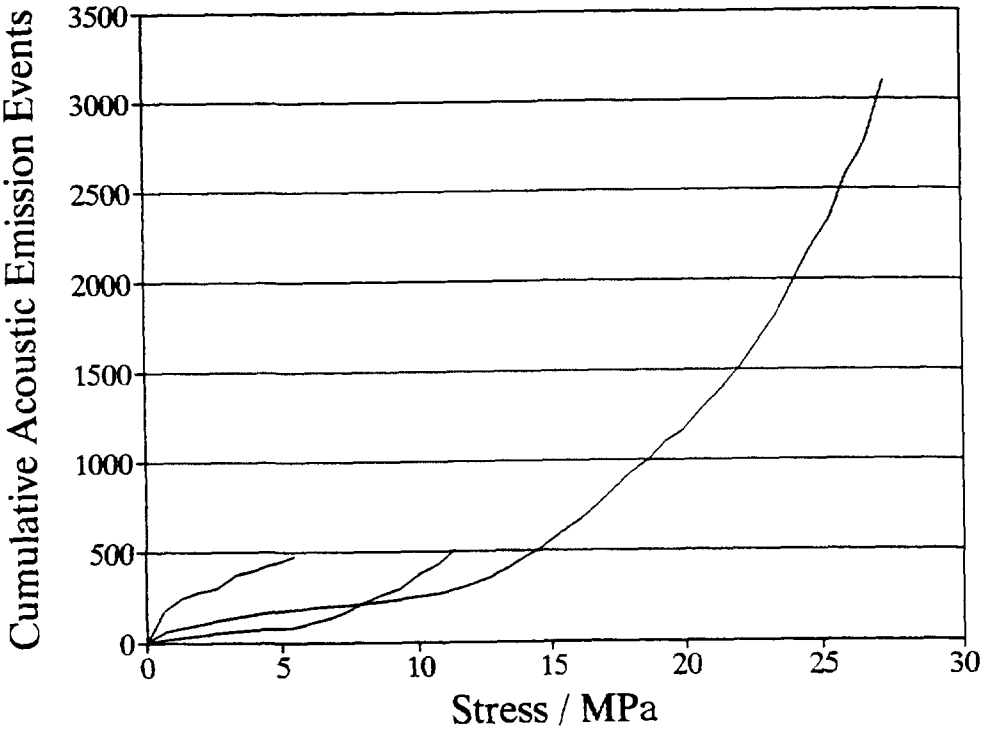

FIGURE 5: Typical example of an AE response from an irradiated graphite specimen subjected to three consecutive load cycles.

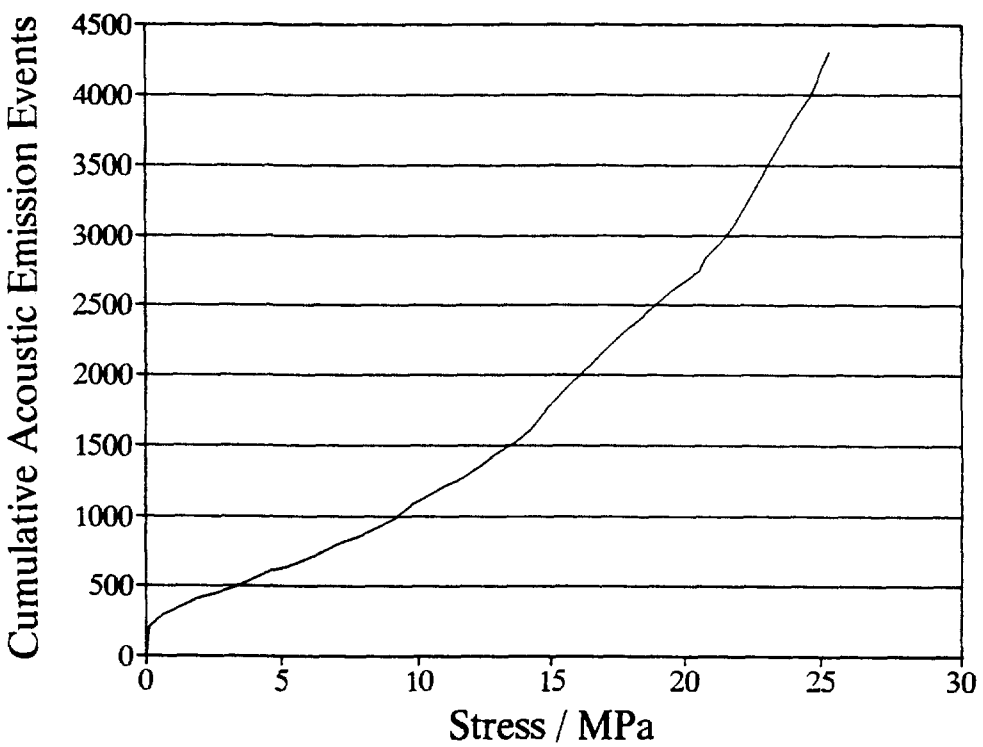

FIGURE 6: An example of an AE response from an irradiated specimen monotonically loaded to failure.

TABLE 4: ΣN at Peak Stresses For Unirradiated and Irradiated Gilsocarbon Graphite.

	Unirradiated						Irradiated					
	Stress / MPa			AE Events			Stress / MPa			AE Events		
	Mean	S.D.	n	Mean	S.D.	n	Mean	S.D.	n	Mean	S.D.	n
First Cycle	4.75	0.57	7	4	4	6	5.3	0.57	6	969	868	5
Second Cycle	9.85	1.35	7	15	8	7	11.12	0.67	6	1532	1061	5
Third Cycle (σ_f)	39.24	3.24	9	967	284	7	27.91	1.72	9	5480	2947	5

Since no evidence for a Felicity effect was revealed, an alternative analysis of the AE data was made by considering a plot of AE event density, *i.e.* the change in ΣN for each stress increment, $\Delta(\Sigma N)/\Delta\sigma$) vs stress, σ. For irradiated graphites, it was postulated that a change in slope in the plot of the AE event density vs stress, marked the position of the internal stress experienced in the reactor. In order to identify the point at which the change in slope of the AE event density-stress curve occurred, a simple empirical analysis was used. It is assumed that the AE event density response is composed of two parts. For stresses, σ, below the pre-stress, σ_p, the AE event density is assumed to be constant with stress, while at stresses greater than σ_p, $\Delta\Sigma N/\Delta\sigma$, is assumed to increase linearly, *i.e.*

$$\Delta(\Sigma N)/\Delta\sigma = a \qquad \sigma < \sigma_p \qquad \text{Eqn. (5)}$$

$$\Delta(\Sigma N)/\Delta\sigma = a + b(\sigma-\sigma_p) \qquad \sigma > \sigma_p \qquad \text{Eqn. (6)}$$

where a and b are constants. The results from irradiated graphite were fitted to the above equations using a least squares best fit method. The values of a, b and σ_p, Table 5, show that there is a wide variation in the parameters a and b for the three irradiated graphites. The values of σ_p for the three graphites lie in the range 4 - 17 MPa and each is significantly different from the others (95% confidence). The mean internal stresses of the specimens generated in-reactor were previously measured by a slot closure technique [19]. Measurements of the internal stresses by slot closure on the sleeve graphite are summarised in Table 6.

TABLE 5: Constant in Equation (6) Fitted to the AE Density Curves for the Irradiated Samples

Sample	a ± 1 S.D.	b ± 1 S.D.	σ_p ± 1 S.D.
612/4/5/6	27.4 ± 2.0	4.0 ± 0.5	4.4 ± 1.9
612/4/3/5	47.9 ± 2.0	10.0 ± 1.2	9.0 ± 1.0
612/7/4/1	37.3 ± 5.5	11.1 ± 2.7	17.0 ± 1.5
Unirradiated	~25	~12.5	~12.0

TABLE 6: Calculated Hoop Stress and Associated Data For Elements 4 and 7 Using the Slot Closure Technique.

Designation	Static Unirradiated Young's Modulus/GPa	Mean Element Burn-up (GWd/t_eU)	Unirradiated Flexural Strength (4pt) / MPa	Internal (Hoop) Stress / MPa
Element 4	9.63	24.24	41.1	2.89 ± 0.38
Element 7	9.63	19.05	41.1	5.16 ± 0.32

Comparison of σ_p values in Table 5 and the internal hoop stresses in Table 6 show that two of the values of σ_p derived from the AE technique, are considerably larger than the hoop stresses obtained from the slot closure method. Considering the empirical nature of the method of identifying σ_p using the AE technique, it seems likely that the internal stress values obtained from the AE method are not associated with irradiation induced internal stresses. Certainly, more work is required before the AE method can be regarded as a reliable one. Further details of these experiments can be found in [15].

4. SUMMARY AND CONCLUSIONS

This paper has presented an overview of a study of the use of AE to monitor residual stresses in moderator graphites using the Kaiser Effect. For several graphite types subject to a wide variety of cyclic loading conditions, AE responses did not exhibit a Kaiser Effect, but instead a Felicity Effect was observed, *i.e.*, the onset of AE occurred below the previously applied peak stress. The Felicity Effect was attributed to time-dependent relaxation and recovery processes at room temperature and was characterised using the Recovery ratio, B. It was shown that AE can be used to monitor creep strain and creep recovery in graphites at zero load. The AE-time responses from these experiments were fitted to equations similar to those used for creep strain-time at elevated temperatures. These results show that there are both time-dependent and time-independent processes which contribute to recovery in polycrystalline graphites.

The AE responses from irradiated fuel sleeve graphites after a full life time subjected to cyclic loading showed a Felicity Effect similar to that shown by unirradiated graphites, except that ΣN values were much greater due to increased porosity resulting from radiolytic oxidation. In addition, irradiated graphites emitted a greater proportion of AE on subsequent load cycles. The AE results from irradiated graphite monotonically loaded to failure revealed no evidence for residual stresses, *i.e.* no Felicity Effect was observed. Residual stresses estimated from the change in the rate of AE with applied stress did not agree with values of internal stress determined by a slot closure method. It is concluded that AE is not a reliable method for estimating residual stresses in moderator graphites, although the use of AE as a tool to investigate relaxation and recovery mechanisms has been clearly demonstrated.

ACKNOWLEDGEMENTS

We thank Berkeley Technology Centre (BTC) of Nuclear Electric plc and the former SERC for their financial support. We would also like to thank BTC for the use of their facilities for some of the work described in this paper.

REFERENCES

1. Andrew, JF, Okada, JW and Wobshall, DC (1960). Proc. 4th Biennial Carbon Conf., Pergammon Press, NY, 559-575.
2. Gilchrist, KE and Wells, D (1969). *Carbon*, 7, 627-631.
3. Kraus, G and Semmler, J (1978). *Carbon*, 16, 185-190.
4. Oakden, MM and Cotten, R (1988). Proc. Carbon '88, Institute of Physics, Bristol, 440-442.
5. Burchell, TD, Cooke, RG, McEnaney, B and Pickup, IM (1985). *Carbon*, 23, [6], 739-747.
6. Burchell, TD (1986). PhD Thesis, University of Bath.
7. Burchell, TD, Rose, APG and McEnaney, B (1986). *J Nucl. Mater.*, 140, 11-18.

8. Ioka, I, Yoda, S, Oku, T and Miyamoto, Y (1986). IAEA Spec. Meet. Graphite Compon. Struct. Des., 227-232, NIPPON Gensuiryowu Rep JAERI M86192.
9. Ioka, I and Yoda, S (1987). *J. Nucl. Mater.*, 148, 344-350.
10. Ioka, I, Yoda, S and Komishi, T (1990). *Carbon*, 28, [4], 489-495.
11. Ioka, I and Yoda, S (1990). *Carbon*, 28, [1], 159-164
12. Neighbour, GB (1993). PhD Theses, University of Bath.
13. Neighbour, GB, McEnaney, B and Phillips, MG (1992). *Carbon*, 30, [3], 359-363.
14. Neighbour, GB and McEnaney, B (1994). *Carbon*, 32, [4], 553-558.
15. Neighbour GB and McEnaney B (1995). *J. Nucl. Mater.*, 223, 305-311.
16. ASTM E-7 Proposal P199.
17. McLachlan, N, Tucker, MO and Parry, MJ (1989). 19th Biennial Conf. on Carbon, Penn. State Uni., 460-461.
18. Davidson, HW and Losty, HHW (1958). *Nature*, 181, 1057-1059.
19. Reed, J, Swallow, K and Neighbour, GB (1991). Private Communication.